Macromolecules

Volume 36, Number 23 November 18, 2003

Communications to the Editor

Dewetting and Layer Inversion of Inverted PVP/PS Bilayer Films

Huiman Kang, Seung-Heon Lee, Sangcheol Kim, and Kookheon Char*

School of Chemical Engineering and Institute of Chemical Processes, Seoul National University, Seoul 151-744, Korea

Received April 3, 2003
Revised Manuscript Received October 4, 2003

The phase separation in polymer blend thin films has extensively been studied due to its importance in polymer coatings and adhesives. The morphology, miscibility, and kinetics of the phase separation in these thin films have been reported to be significantly different from those in bulk due to their confined nature between the air and the substrate.[1−3] The constituent polymers in a polymer blend thin film tend to segregate *asymmetrically* or *symmetrically* to polymer/air and polymer/substrate interfaces according to the interplay between their surface tensions and their affinity to the substrates.[1,2] In the case where blend components segregate asymmetrically to each interface, the blend film eventually stratifies into a bilayer when phase separation occurs. In contrast, when a blend component is preferred at both interfaces, the blend film in equilibrium state shows the symmetric segregation of the component toward both interfaces with the other component sandwiched between them.[2,3]

Polymer blend thin films can be easily prepared by spin-casting using a common solvent. Since polymers in blends are generally quite immiscible owing to the entropic nature of long chains, the phase separation often occurs during the spin-coating procedure. The phase-separated domain morphology formed during the solvent evaporation has commonly been observed on the surface of as-cast polymer blend thin films.[4,5] Poly(2-vinylpyridine) (PVP) and polystyrene (PS) are one of the most immiscible pairs,[6] and the phase separation immediately starts as soon as a PVP/PS blend thin film is spin-coated on a silicon wafer with a native silicon oxide on top.[4] When the film is annealed above the glass transition temperatures of both PS and PVP, asymmetric segregation occurs leading to the bilayer of PS and PVP since PVP has a strong enthalpic affinity for the silicon oxide while PS preferentially wets the air/polymer interface due to its lower surface energy. However, studies of the phase separation in PVP/PS blend thin films have been quite limited due to the phase-separated structures of as-cast films.

In this study, the PVP/PS bilayer films with a PS layer on the silicon wafer and a PVP layer on top of the PS layer were prepared by a sequential spin-coating procedure using different solvents for both PS and PVP to prevent the initial phase separation of PVP/PS blend thin films. These films will be denoted hereafter as *inverted* PVP/PS bilayer films because they have an inverted structure against a thermodynamically preferred sequence with a PS layer on the surface and a PVP layer on the silicon wafer. When the inverted bilayer films were annealed above the glass transition temperatures of both components, dewetting occurred at the polymer/polymer interface (liquid/liquid dewetting), and finally the partial layer inversion was achieved. Optical (OM) and atomic force microscopies (AFM) were employed to investigate the surface and interface morphologies of the inverted PVP/PS bilayer films as a function of annealing temperature and time.

Monodisperse PS and PVP were synthesized by anionic polymerization in high vacuum using a glass-blowing technique. The polymerizations of PS and PVP were initiated in benzene by *n*-BuLi and in THF by *sec*-BuLi, respectively, and terminated by methanol. The molecular weights (M_n, M_w) and polydispersity indexes (M_w/M_n) of the polymers synthesized were determined by GPC using PS standards. The glass transition temperatures (T_g) of PS and PVP were measured by a differential scanning calorimeter (DSC2010, TA Instruments). RMS 800 (Rheometric Scientific Inc.) in parallel plate geometry with 25 mm diameter and 1.5 mm gap

* To whom correspondence should be addressed. E-mail: khchar@plaza.snu.ac.kr.

10.1021/ma034421n CCC: $25.00
Published on Web 10/18/2003

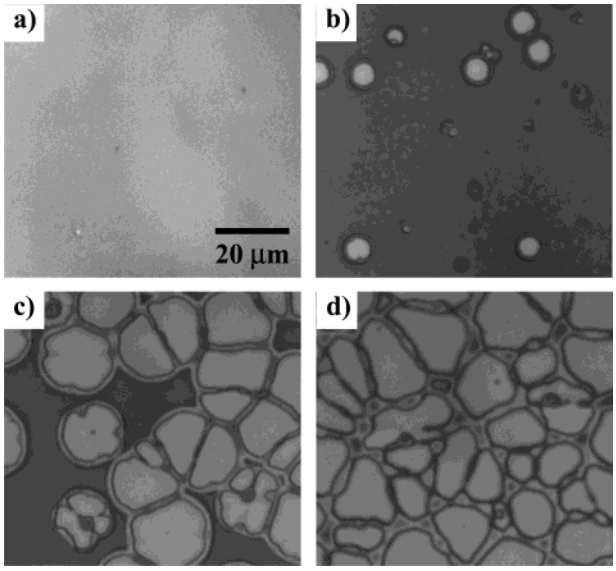

Figure 1. Optical micrographs for (a) an as-cast PVP/PS bilayer film and PVP/PS bilayer films annealed at 130 °C for (b) 3, (c) 5, and (d) 10 min.

Table 1. Characteristics of Polymers Used in the Present Study

polymer	M_n (g/mol)	M_w (g/mol)	M_w/M_n	T_g (°C)	η_0 (Pa s) at 130 °C	η_0 (Pa s) at 190 °C
PS	11700	12300	1.05	96	10000	8
PVP	7900	8100	1.03	95	32 000	32

was employed to measure the zero shear viscosities of PS and PVP. Table 1 summarizes the characteristics of polymers used in present study.

The inverted PVP/PS bilayer film was prepared by sequential spin-coating. A thin PS film was first spun-cast from 1 wt % solution in toluene at 2000 rpm onto a silicon wafer with a native oxide layer (~30 Å), which was pretreated with piranha solution. A 1 wt % PVP solution in methanol was then spun-coated at 2000 rpm on top of the as-cast PS film. We note that the spin-casting of the upper PVP layer with methanol does not affect the homogeneity of the bottom PS film since methanol is a nonsolvent for PS. It was confirmed that the interface of the as-cast PVP/PS bilayer film was flat and smooth. The thickness of each layer was measured to be about 40 nm using a Gaertner ellipsometer with a He−Ne laser with $\lambda = 632.8$ nm. The bilayer films were annealed under vacuum at 130 or 190 °C, which is well above the glass transition temperatures of both PS and PVP.

The surface morphology and dewetting process of the inverted PVP/PS bilayer films were investigated as a function of annealing time and temperature by using OM and AFM. OM measurements were carried out using a Nikon OPTIPHOT2-POL in reflection mode. AFM measurements were performed using a Digital Instruments Nanoscope IIIa with a Si_3N_4 tip in contact mode.

Figure 1 shows the optical micrographs for the dewetting morphology of an inverted PVP/PS bilayer film on a silicon wafer substrate while annealing at 130 °C. The surface morphology of the as-cast PVP/PS bilayer film is featureless as expected (Figure 1a). Annealing at 130 °C, however, induces the dewetting of the upper PVP layer from its lower PS layer. The dewetted PVP holes with rims are clearly observed in Figure 1b after 3 min of annealing. These dewetted holes grow with time, and the hole rims merge with one another when annealed at 130 °C for 5 min (Figure 1c). After 10 min of annealing, a polygonal network pattern is observed (Figure 1d), which is the characteristic dewetting morphology in the late stage.

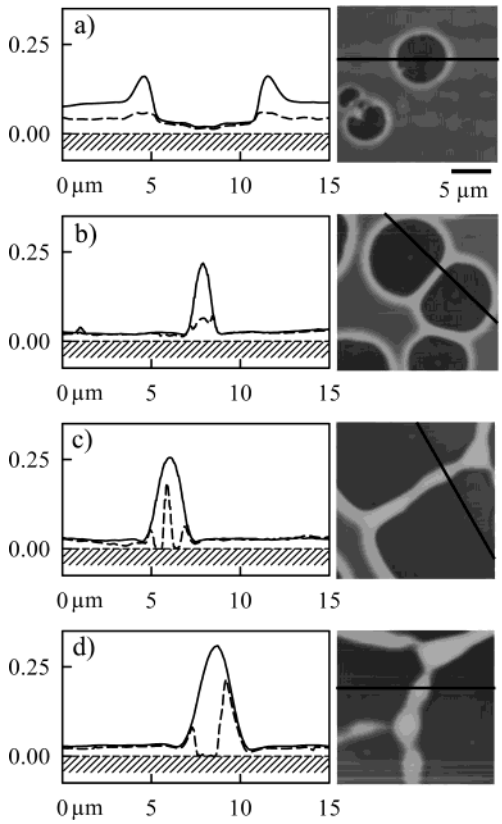

Figure 2. AFM height images and cross-sectional height profiles for the surface of PVP/PS bilayer films annealed at 130 °C for (a) 3, (b) 5, (c) 6, and (d) 13 min. A cross-sectional height profile locating the interface of PVP/PS bilayer films obtained after the upper PVP layer was washed off by PVP selective methanol is also shown as a dashed line in each profile. The substrate is also indicated in each profile for clarity.

To investigate the dewetting mechanism of *inverted* PVP/PS bilayer films, we examined both surface and interface morphologies of the films during the early stage of annealing using AFM. Figure 2 shows the AFM height images and cross-sectional height profiles for the surface (solid lines) of PVP/PS bilayer films annealed at 130 °C for (a) 3, (b) 5, (c) 6, and (d) 13 min. The interface morphologies of the same regions were also checked by AFM after washing off the upper PVP layer by methanol, which is solely selective to PVP, thus enabling us to monitor the lower PS layer. The respective cross-sectional height profiles obtained for the interface of PVP/PS bilayer films are also shown as dashed lines in the figures. The silicon substrate is also indicated in each profile for clarity. As annealing proceeds through 3 min, the upper PVP layer dewets from the lower PS layer, and the dewetted holes are simultaneously created at the surface of PVP/PS bilayer film (Figure 2a). In Figure 2a, the interfacial morphology resembles the dewetted pattern of the upper PVP layer, and two profiles exactly match with each other in the hole region, implying that the upper PVP layer dewets the lower PS layer. It should be noted here that the dewetting of PVP on PS induces fluctuation in film thickness at the PVP/PS interface since PS has a lower

viscosity than PVP. Although the molecular weight of PVP is slightly smaller than that of PS, its zero shear viscosity is about 3.2 times larger than that of PS at 130 °C, as shown in Table 1.

According to several reports on the liquid/liquid interface dewetting, for a *solidlike* (highly viscous) lower layer, a dewetted upper layer does not affect the lower layer while, for a *liquidlike* (less viscous) lower layer, the dewetting causes a lift-up of the lower layer at the initial stage.[7−10] Qu et al.[8] investigated the liquid/liquid dewetting dynamics of a PS layer on top of a poly(methyl methacrylate) (PMMA) layer and observed the fluctuation and the thinning in the lower layer of the dewetted region similar to our profile shown in Figure 2a when the lower PMMA layer has much lower molecular weight than the upper PS layer. They further reported that, for high PMMA molecular weights, the PS dewetting velocity scales inversely with the PS viscosity while, for low PMMA molecular weights, the dewetting velocity is almost independent of the PS viscosity. Segalman and Green[9] also reported similar fluctuation and thinning in the lower layer during the dewetting of a high molecular weight PS on a low molecular weight poly(styrene-*co*-acrylonitrile) (SAN). All the previous results along with current results imply that the dewetting kinetics and the surface morphology in liquid/liquid dewetting system mainly depends on the viscosity difference of constituent polymers as well as individual layer thickness.[8−10]

After the dewetted holes are created, the dewetting of inverted PVP/PS bilayer films further progresses with the growth of the holes and the merging of the rims due to the collision of adjacent holes, resulting in a connected hole structure (Figure 2b). The film finally builds up a polygonal network over the whole surface area (Figure 2c,d). With regard to the surface morphology, the PVP dewetting in the inverted PVP/PS bilayer film (liquid/liquid dewetting) is quite similar to the dewetting of a single polymer thin film on a nonwettable substrate (liquid/solid dewetting). The dewetting process of a polymer thin film on a nonwettable substrate is known to proceed in three characteristic steps:[11,12] first, the polymer film ruptures and the dewetted holes with elevated rims are simultaneously created. Second, these holes grow with time until the rims merge and build up a polygonal network over the whole surface of a substrate. Finally, this network system of the dewetted polymer film transforms into droplets due to the capillary instability. The droplet formation, however, was not observed to occur in our case due to the fact that the *layer inversion* starts in our system through the migration of the dewetted PVP in the merged rims down to the silicon substrate. This will be discussed in detail below.

It is interesting to note in Figure 2b that the interface profile at 5 min reveals both the ridge and the central mound, which is composed of PS, in the merged rims. This intriguing interfacial shape is due to the merging of two rims. In Figure 2c, as the merging of two rims proceeds further, the height of the central mound in the interface profile as well as the total height of the merged rims increases, and both ridges move down to the silicon substrate with one ridge finally contacting the substrate due to the higher affinity of PVP toward the substrate. After the PVP layer touches the substrate in the merged rim, more PVP chains are allowed to easily spread into the contact area on the substrate, and this process

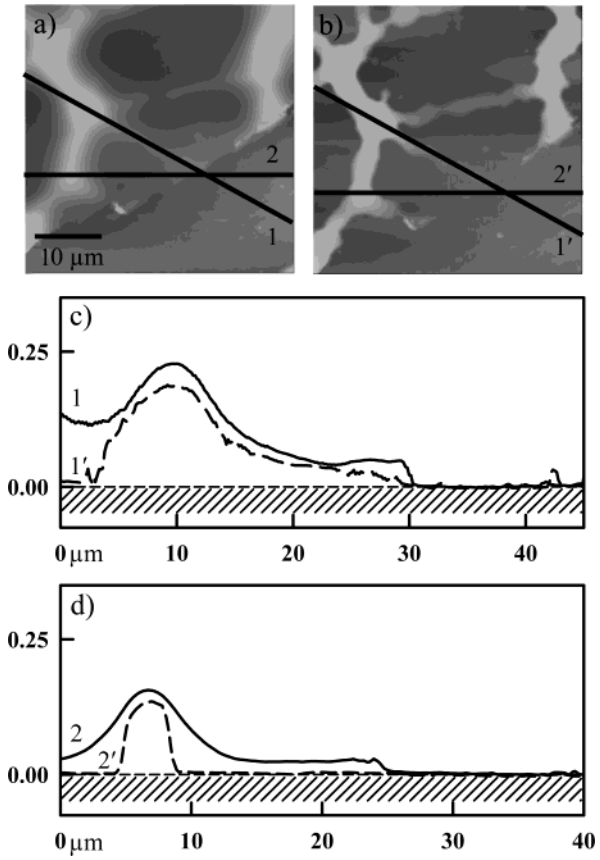

Figure 3. AFM height images for the scratched region of an inverted PVP/PS bilayer film annealed at 190 °C for 156 h (a) before and (b) after the film was treated with PS selective cyclohexane. (c) Cross-sectional height profiles for line 1 in (a) (solid line) and line 1′ in (b) (dashed line). (d) Another cross-sectional height profiles for line 2 in (a) (solid line) and line 2′ in (b) (dashed line). The substrate is also indicated in each cross-sectional profile for clarity.

expels the PS chains in the central mound toward the walls of the rim. Finally, at 13 min, the central mound in the PS layer vanishes, and PS is concentrated at both walls of the rims as shown in Figure 2d. The distribution of PS along both walls of the rim is highly asymmetric as shown in Figure 2d, which supports the above argument.

Prolonged annealing over 13 min at 130 °C did not change the dewetted morphology of the PVP/PS bilayer films further probably due to the low chain mobilities since the annealing temperature is not far from the glass transition temperatures of both polymers. To investigate the equilibrium structure of inverted PVP/PS bilayer films after the dewetting process, the as-cast specimen was annealed at a higher temperature of 190 °C for a long time.

Figure 3a shows the AFM height image for a PVP/PS bilayer film annealed at 190 °C for 156 h. A scratch with a clean knife was performed on the film as shown in lower right region of Figure 3a in order to obtain information on the film thickness. The morphology of the fully annealed bilayer film remained the same after treating with PVP selective methanol, implying that the whole surface is covered by PS. X-ray photoelectron spectroscopy (XPS) for this sample (data not shown here) also indicated that the surface is composed of PS only. As a result, we treated the fully annealed bilayer films with PS selective cyclohexane to dissolve the upper PS layer for the study of the interface profile. AFM was

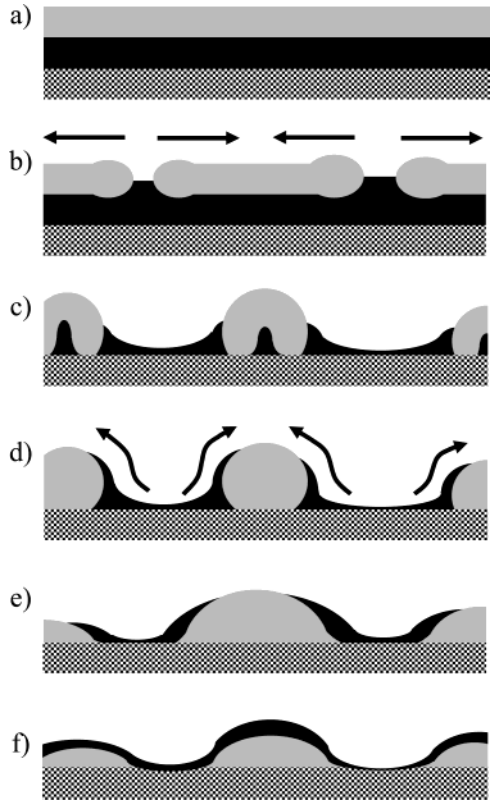

Figure 4. A schematic depicting the dewetting and the layer inversion of enthalpically inverted PVP/PS bilayer films while annealing above the glass transition temperatures of PS and PVP. Each figure explains (a) inverted PVP/PS bilayer film on SiO_2 substrate, (b) creation of dewetted PVP holes with exposure of lower PS layer, (c) mergence of dewetted PVP rims, (d) migration of PVP domains to SiO_2 substrate, (e) PVP domains partly coated with PS on surface, and (f) bilayered film with PS layer on top and PVP layer in contact with SiO_2 substrate.

carefully performed on the same region shown in Figure 3a after washing off the upper PS layer, and the resulting height image is given in Figure 3b. The cross-sectional height profiles for line 1 in Figure 3a and line 1′ in Figure 3b are shown in Figure 3c as solid and dashed lines, respectively. The cross-sectional height profiles for lines 2 and 2′ are also shown in Figure 3d. The silicon substrates are again indicated in Figure 3c,d for clarity. It can be clearly seen in Figure 3c,d that a thin PS layer covers the PVP domains over the entire area examined, implying that the *layer inversion* was achieved. In Figure 3c, the maximum height of the annealed PVP/PS bilayer film is 226 nm and that of washed PVP/PS bilayer film is 183 nm, showing the 40 nm difference in thickness. It should be mentioned here that the layer inversion observed in our system did not occur in the works of Qu et al.[8] and Segalman and Green[9] since the interfacial energy between the lower layer and the silicon oxide is smaller than the interfacial energy between the upper layer and the silicon oxide in their systems.

On the basis of above experimental observations, we propose a schematic, shown in Figure 4, on the dewetting process and the layer inversion of an inverted PVP/PS bilayer film on a silicon wafer if the lower PS layer is less viscous than the upper PVP layer. When the inverted bilayer film in Figure 4a is annealed above their glass transition temperatures, the upper PVP layer first dewets from the lower PS layer (liquid/liquid dewetting) at the initial stage of annealing. Since PVP is more viscous than PS in our system, the dewetting of the upper PVP layer perturbs the lower PS layer to a larger extent and then causes the thinning of the PS layer in dewetted hole region due to the hydrodynamic flow of PVP layer (Figure 4b). As the dewetted PVP holes grow, the hole rims merge with one another, and this process physically confines the lower PS layer to form a mound in the middle and a ridge along the circumference of the rim at the interface (Figure 4c). As the PVP dewetting further proceeds, a polygonal network of the PVP rims is formed, and this confines the PS even further, such that the ridges and the central mound at the interface are more pronounced. A fraction of the ridge finally makes a contact between PVP and the silicon oxide layer on a silicon wafer due to the strong affinity between PVP and silicon oxide (Figure 4c). The central PS mound in the merged rim disappears by the PVP displacing toward the substrate through the contact area and the spreading of PS chains to the rim through the connected PS channels (Figure 4d). Finally, the partial layer inversion occurs with prolonged annealing or high-temperature annealing since the PVP domains in the rims spreads laterally due to their higher affinity toward the substrate (Figure 4e) while the PS chains in contact with the silicon substrate spread along the surface of the PVP domains and finally encapsulate the PVP domains due to their lower surface energy (Figure 4f). A thin PS layer covers the entire surface with a polygonal network of PVP domains in contact with the silicon substrate at the fully annealed state (Figure 4f). A smooth PS/PVP bilayer with PS layer on top and PVP layer at the bottom, which is expected to be an equilibrium morphology,[4] was not observed in our system even after further annealing. Our corrugated surface morphology at the fully annealed state is believed to be in quasi-equilibrium since, unlike low molecular weight molecules, it takes much longer time than the experimentally accessible time scale for the PVP microdroplet in Figure 4d, to spread to form a flat bilayer film.[13] The fact that the PS layer remains in contact with the PVP domains and the substrate, making three-phase contact angle, also contributes to the pinning of the corrugated morphology.

The dewetting and layer inversion process of our inverted PVP/PS bilayer films can be explained quantitatively by using the surface tensions of PS (γ_{PS}) and PVP (γ_{PVP}) as well as the interfacial tensions of PVP/PS (γ_{PS-PVP}), PVP/SiO_x ($\gamma_{PVP-SiO}$), and PS/SiO_x (γ_{PS-SiO}). The surface tensions of PS (γ_{PS}) and PVP (γ_{PVP}) are 32.66 and 38.51 mN/m at 130 °C, respectively, from the extrapolation of the results of Sauer and Dee,[14] and the interfacial tension between PS and PVP (γ_{PS-PVP}) is 3.46 mN/m at 130 °C.[15] The wetting behavior of PVP on PS is described by the spreading parameter defined as $S = \gamma_{PS} - (\gamma_{PVP} + \gamma_{PS-PVP})$. S becomes negative when the values of γ_{PS}, γ_{PVP}, and γ_{PS-PVP} are put into the above equation, which implies that PVP should dewet PS above the glass transition temperatures of constituent polymers. This is in agreement with the observed dewetting behavior in our system. Displacement and spreading of dewetted PVP domains on the silicon oxide substrate occur since $\gamma_{PVP-SiO} < \gamma_{PS-SiO}$ while PS segregates to the air surface since $\gamma_{PS} < \gamma_{PVP}$. This process finally leads to the partial layer inversion.

Recently, Rafailovich and co-workers[16−18] have investigated the dewetting in bilayer films of partially

brominated polystyrene (PBrS) on PS. Although their studies were lack of the kinetics, their final dewetted surface morphology is quite reminiscent of ours shown in Figure 1d. Similar to our study, the upper PBrS layer first dewets the lower PS layer since $S = \gamma_{PS} - (\gamma_{PBrS} + \gamma_{PS-PBrS})$ becomes negative. In their system, however, the symmetric wetting of PS toward both surface and substrate occurs after PBrS dewetting since $\gamma_{PS} < \gamma_{PBrS}$ and $\gamma_{PS-SiO} < \gamma_{PBrS-SiO}$. This symmetric wetting of PS confines the PBrS domains inside the dewetted rims, and the layer inversion observed in our system does not occur.

In summary, we have investigated the kinetics of the dewetting and the layer inversion in enthalpically inverted PVP/PS bilayer films on a silicon wafer during annealing using both OM and AFM. Dissolution of the upper layer by PVP (or PS) selective solvent allowed us to study the interface profiles at different annealing times. It was found that the upper PVP layer first dewets the lower PS layer (*liquid/liquid dewetting*) and that the dewetting follows a mechanism similar to the liquid/solid dewetting until the dewetted PVP holes merge with each other to form a polygonal network structure of the rims although the lower PS layer is slightly deformed by the hydrodynamic flow of the dewetting PVP layer since the PS used in the present study has a lower viscosity than the PVP. After the rims of dewetted PVP holes are merged together, the layer inversion process starts by the contact and the subsequent displacement of PVP toward the substrate due to its higher affinity for the substrate. Partial layer inversion with a thin PS layer on top of the PVP domains is finally achieved after a prolonged annealing (or high-temperature annealing) due to the fact that PS has a lower surface energy. We expect that the dewetting and the layer inversion in inverted PVP/PS bilayer films are considerably different depending on the molecular weights of polymers used and the thickness of each layer. The detailed studies on these issues, however, are beyond the scope of this paper and will be discussed in future publications.

Acknowledgment. We thank Prof. E. J. Kramer at UCSB for thoroughly reading the manuscript and providing valuable suggestions. This work was supported by the National Research Laboratory fund (Grant M1-0104-00-0191) from the Ministry of Science and Technology (MOST), the Ministry of Education through the Brain Korea 21 Program at Seoul National University, and the National R&D Project for Nano Science and Technology from MOST.

References and Notes

(1) Ermi, B. D.; Karim, A.; Douglas, J. F. *J. Polym. Sci., Part B: Polym. Phys. Ed.* **1998**, *36*, 191.
(2) Karim, A.; Slawecki, T. M.; Kumar, S. K.; Douglas, J. F.; Satija, S. K.; Han, C. C.; Russell, T. P.; Liu, Y.; Overney, R.; Sokolov, J.; Rafailovich, M. H. *Macromolecules* **1998**, *31*, 857 and references therein.
(3) Keblinski, P.; Kumar, S. K.; Maritan, A.; Koplik, J.; Banavar, J. R. *Phys. Rev. Lett.* **1996**, *76*, 1106.
(4) Boltau, M.; Walheim, S.; Mlynek, J.; Krausch, G.; Steiner, U. *Nature (London)* **1998**, *391*, 877.
(5) Walheim, S.; Boltau, M.; Mlynek, J.; Krausch, G.; Steiner, U. *Macromolecules* **1997**, *30*, 4995.
(6) Dai, K.; Kramer, E. J. *Polymer* **1994**, *35*, 157. The temperature-dependent Flory−Huggins interaction parameter $\chi(T)$ for PS−PVP is given by $\chi(T) = -0.033 + (63/T)$. Therefore, their χ is 0.123 at 130 °C.
(7) Faldi, A.; Composto, R. J.; Winey, K. I. *Langmuir* **1995**, *11*, 4855.
(8) Qu, S.; Clarke, C. J.; Liu, Y.; Rafailovich, M. H.; Sokolov, J.; Phelan, K. C.; Krausch, G. *Macromolecules* **1997**, *30*, 3640.
(9) Segalman, R. A.; Green, P. F. *Macromolecules* **1999**, *32*, 801.
(10) Lambooy, P.; Phelan, K. C.; Haugg, O.; Krausch, G. *Phys. Rev. Lett.* **1996**, *76*, 1110.
(11) Brochard-Wyart, F.; Daillant, J. *Can. J. Phys.* **1990**, *68*, 1084.
(12) Reiter, G. *Phys. Rev. Lett.* **1992**, *68*, 75.
(13) Fraysse, N.; Valignat, M. P.; Cazabat, A. M.; Heslot, F.; Levinson, P. *J. Colloid Interface Sci.* **1993**, *158*, 27. Valignat, M. P.; Fraysse, N.; Cazabat, A. M.; Heslot, F. *Langmuir* **1993**, *9*, 601. Valignat, M. P.; Oshanin, G.; Villette, S.; Cazabat, A. M.; Moreau, M. *Phys. Rev. Lett.* **1998**, *80*, 5377. Voue, M.; Valignat, M. P.; Oshanin, G.; Cazabat, A. M. *Langmuir* **1999**, *15*, 1522.
(14) Sauer, B. B.; Dee, G. T. *Macromolecules* **2002**, *35*, 7024.
(15) Helfand, E.; Tagami, Y. *Polym. Lett.* **1971**, *9*, 741.
(16) Slep, D.; Asselta, J.; Rafailovich, M. H.; Sokolov, J.; Winesett, D. A.; Smith, A. P.; Ade, H.; Anders, S. *Langmuir* **2000**, *16*, 2369.
(17) Slep, D.; Asselta, J.; Rafailovich, M. H.; Sokolov, J.; Winesett, D. A.; Smith, A. P.; Ade, H.; Strzhemechny, Y.; Schwars, S. A.; Sauer, B. B. *Langmuir* **1998**, *14*, 4860.
(18) Ade, H.; Winesett, D. A.; Smith, A. P.; Anders, S.; Stammler, T.; Heske, C.; Slep, D.; Rafailovich, M. H.; Sokolov, J.; Stöhr, J. *Appl. Phys. Lett.* **1998**, *73*, 3775.

MA034421N